



Journal of Mining and Earth Sciences

Website: <http://jmes.humg.edu.vn>



Resection method for direct georeferencing in Terrestrial Laser Scanner



Dung Trung Pham ^{1,*}, Anh Tuan Nhu Nguyen ², Cuong Xuan Cao ¹,
Tinh Duc Le ¹, Canh Van Le ¹, Cuong Sy Ngo ³

¹ Hanoi University of Mining and Geology, Hanoi, Vietnam

² Topcon Singapore Positioning Pte. Ltd Singapore, Ho Chi Minh City, Vietnam

³ Vietnam Natural Resources and Environment Company, Hanoi, Vietnam

ARTICLE INFO

Article history:

Received 05th Jan. 2022

Revised 16th Apr. 2022

Accepted 30th May 2022

Keywords:

Cloud-to-Cloud method,
Direct georeferencing,
Incidence angle,
Resection method,
Terrestrial laser scanner.

ABSTRACT

Recently, the direct georeferencing method has been increasingly used in Terrestrial Laser Scanner (TLS). This method has the benefit of saving time, but the low accuracy is a great difficulty to use. This paper proposed a possible approach for direct georeferencing with high accuracy using the resection method. Thanks to new series of TLS combined with a total station called the total station scanner, the resection method can be applied to overcome the problem. However, the assessment of the resection method on the quality of the point cloud is lacking up to now. In this paper, the influence of components of error sources in the resection method on the total error of the point cloud is analyzed. In the experiment, a Topcon GTL-1000 total station scanner was employed. A ground control network and checkered targets were established by a Leica TS06 plus total station. The experimental results verify that the total error of point cloud entirely agrees with the theory about georeferencing using the resection method. In addition, the distance and incidence angle from the scanner to the measured object are the main factors that considerably influence the accuracy of the point cloud. The relationship between these factors and the accuracy of the point cloud is non-linear measured by a coefficient of determination ($R^2 > 0.7$). Using the resection method, the coordinates of the scan station can obtain at a millimeter level in accuracy. As a result, the resection method is one of the most suitable methods that can be applied for georeferencing in TLS. The high accuracy and saving time for TLS data post-processing in the office are enormous benefits of this method.

Copyright © 2022 Hanoi University of Mining and Geology. All rights reserved.

*Corresponding author

E - mail: phamtrungdung@humg.edu.vn

DOI: 10.46326/JMES.2021.63(3).07

1. Introduction

Georeferencing is a process of transformation between a local and global coordinate system in Figure 1. For the TLS survey, the local and global coordinate systems are called Intrinsic Reference Systems (IRS) and Ground Control Point (GCP), respectively.

The transformation to a global coordinate system VN2000 is applied by a 3D-Helmert transformation. Since the scale is known, the transformation requires six parameters that are three translations $X_{Scanner}$ and three rotations (α, θ, κ) . The transformation from the local system to the global system (VN2000) or ground control points (GCPs) is represented by the equation (Hofmann-Wellenhof et al., 2007):

$$X_{object} = X_{Scanner} + R_{IRS}^{GCP}(\alpha, \theta, \kappa)x_{IRS}, \quad (1)$$

Where R_{IRS}^{GCP} is the rotation matrix around the x-, y-, and z-axis, respectively. X_{object} and $X_{Scanner}$ are coordinates of object and scanner in GCP, correspondingly. x_{IRS} is the coordinates of the object in IRS.

Georeferencing can be performed in two common ways of direct and indirect methods (Lichti and Gordon, 2004).

Indirect georeferencing uses known points of makers or targets to georeference the point cloud. These points have global coordinates and they are

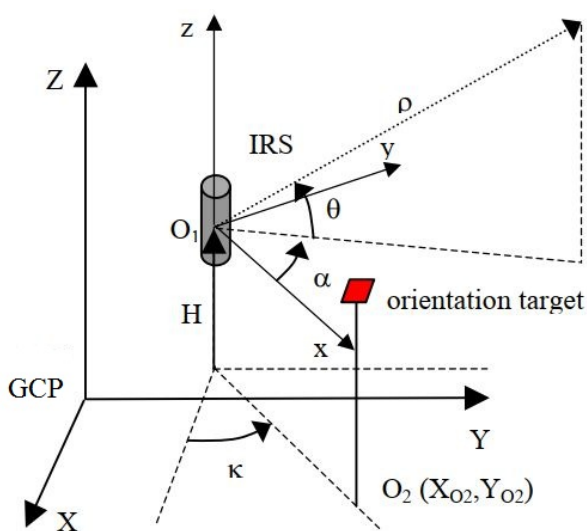


Figure 1. Transformation between global and local coordinates (Scaioni 2005).

also measured in the local coordinates by the scanner, thus the transformation parameter can be estimated by indirect georeferencing. By contrast, indirect georeferencing requires at least three known GCPs in each scan. In Vietnam, due to the separation of horizontal and vertical control networks, the information of these control points needs to be transferred to the targets by geodetic methods, such as a total station, RTK-GNSS. The advantage of the indirect method is that a plumbing scanner is not required. In addition, the scan station is arbitrary around the scanning object. Moreover, the height instrument is not necessary to measure when a checkered target is on the wall. The neglect of the determination of the height of both instrument and checkered target allows high accuracy in the indirect georeferencing method to be obtained. Alternatively, georeferencing can be realized using surfaces or building models (Schuhmacher and Böhm, 2005). One of the greatest disadvantages of indirect georeferencing is the need for a second instrument to measure the position of GCPs. Additionally, other equipment such as checkered targets must be placed as tie points around the object. As a result, indirect georeferencing is very time-consuming and costly.

Direct georeferencing is a method that can save time and cost since both the scan station and the oriented target can be automatically located in the global coordinate. The coordinate of both the scanner and its corresponding target can be determined by a low-cost GNSS receiver that is centered close to the scanner's rotation axis (Zimmermann et al., 2018). Since these coordinates can be measured before/after or parallel to scanning time, the scanning can be processed in real-time. The considerable advantage of direct georeferencing is that the time for data post-processing in the office can be considerably reduced. However, the main drawback of this method is the positional accuracy of the scan station and target measured by GNSS absolute positioning, normally a meter-level accuracy. If the GNSS real-time kinematic (RTK) is applied, the accuracy is improved to a centimeter-level in horizontal coordinates. Furthermore, direct georeferencing is not suitable in some applications because of the multipath

effect in GNSS. For example, scanning is carried out in the city, especially in indoor applications or tunnels.

In the direct georeferencing method, Altuntas et al. (2014) proposed a method for georeferencing in which two GNSS receivers are used. One receiver is mounted in the scanner and another is used for the target. The position of both the scan station and target can be determined by GNSS after a few minutes. Moreover, Jaud et al. (2017) developed the pseudo-direct georeferencing method, a simple and quick method. An internal inclinometer to measure roll and pitch angles and a centimetric GNSS-RTK for positioning of both scan station and backsight target are involved in this method. This method is much quicker than the classical indirect georeferencing method and it proved to be more precise than indirect georeferencing. The accuracy of the pseudo-direct method can obtain root mean square errors (RMSE) of 3.8 cm.

Currently, the existing scanners can operate as a total station. The scanner is mounted over a tribrach and center over a known point. A telescope is also provided for backsighting a target for orientation in horizontal coordinates. In this paper, a georeferencing method is applied resection function of GTL-1000 to get the coordinates of the scan station. However, up to now, there is no comprehensive evaluation of the resection method in direct georeferencing for TLS. The paper aims to assess the effect of component error sources in the resection method on the total error of the point cloud. Besides, the influence of distance and incidence angle on the quality of point cloud is considered.

The paper is divided into six sections. The principle and error sources of the resection method used for direct georeferencing are described in section 2. Section 3 presents the experiment of the resection method used for TLS. The results and discussions of the paper are described in sections 4 and 5, respectively. The conclusion of the paper is summarized in the last section.

2. Direct georeferencing by resection method

2.1. Resection method in TLS

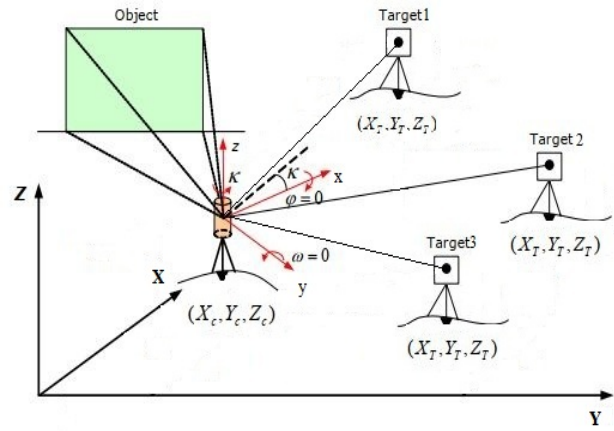


Figure 2. Geometry of resection method in TLS.

Space resection or 3D resection is one of the methods that can be applied for direct georeferencing. 3D resection is used to locate an unknown of a scan station $X_{scanner}$ in (1). In practice, to determine the coordinate in 3D of the scan station, three or more targets are usually used (Figure 2). The unknown coordinate of the scan station is determined by observations of a range (ρ), a horizontal rotation angle (α), and a vertical attitude angle (θ) in cartesian coordinates (x, y, z). The relationship between observations and coordinates is given as:

$$\begin{pmatrix} x \\ y \\ z \end{pmatrix} = \begin{pmatrix} \rho \sin \alpha \cos \theta \\ \rho \sin \alpha \sin \theta \\ \rho \cos \alpha \end{pmatrix} \quad (2)$$

The geometry of resection is shown in and the functional model for 3D resection is given as:

$$\begin{pmatrix} x \\ y \\ z \end{pmatrix} = R_{IRS}^{GCP} \begin{pmatrix} X - x_{IRS} \\ Y - y_{IRS} \\ Z - z_{IRS} \end{pmatrix} \quad (3)$$

Because almost all scanners are equipped with a dual-axis compensator, the angles α , and ω are assumed to be zero when the scanner is levelled. Thus the rotation matrix R_{IRS}^{GCP} is a function only of the azimuth (κ) that can be written as:

$$R_{IRS}^{GCP} = \begin{pmatrix} \cos \kappa & \sin \kappa & 0 \\ -\sin \kappa & \cos \kappa & 0 \\ 0 & 0 & 1 \end{pmatrix} \quad (4)$$

2.2. Errors in georeferencing by resection

Because the resection approach is one of the methods for direct georeferencing, the error of this approach can be analyzed based on the direct georeferencing method. The error source in direct georeferencing can be classified into five components as follows (Lichti and Gordon, 2004):

- The positional errors of survey station and backsight target;
- The centering and levelling errors of the scanner;
- The centering error of backsight target (It is noted that the centering error of backsight target can be neglected if markers are used);
- The measurement errors of the scanner;
- Laser beam width.

The rest of the subsection will be analyzed in more detail as follows:

In the first components, the covariance matrices of scanner position and backsight target are denoted by $C_{scanner}$ and C_{BS} . The $C_{scanner}$ contributes by covariances of scanner position C_0 and the vertical position determined by tape or laser range C_H , $C_{scanner}=C_0+C_H$. The accuracy of positional scan station C_0 depends on the quality of the control network. The accuracy of determination of orientation from scanner to backsight target is:

$$\sigma_{\kappa} = \pm \frac{\sqrt{2}\sigma_{hor}}{r} [rad] \quad (5)$$

Where: σ_{hor} is the accuracy of horizontal angle and r is the range from the scanner to the backsight target.

The second and third components contribute by the centering error of scanner and backsight target and scanner levelling. The centering error is given as:

$$\sigma_{cent} = \pm \frac{\sqrt{2}\sigma_{oc}}{r} [rad] \quad (6)$$

With σ_{oc} is the centering accuracy.

The azimuth accuracy is inversely proportional to the range between the scan station and the target:

$$\sigma_A = \pm \frac{\sqrt{2}\rho\sigma_H}{r} \quad (7)$$

Where σ_H is the error of horizontal coordinate.

It is worth noting that, the manual point collimation to the backsight targets in the

resection method is done at least two times (practically three or more times). In addition, if the targets are markers on the wall, the centering error of the backsight targets can be neglected.

The levelling error in the vertical and horizontal angles is estimated by $\sigma_{lv} = \pm 0.2v$ and $\sigma_{lh} = \pm \sigma_{lv} \tan \theta$, respectively where v is the sensitivity of the scanner level bubble (in radians). Currently, the scanner is equipped with a dual-axis compensator with 0.015° of accuracy in a range of $\pm 5^\circ$, so this error source is very small. The pointing to the backsight target with a telescope is $\sigma_p = \pm 60''/M$ where M is the telescope magnification. The covariance matrix C_{set} of the setup errors is given as:

$$C_{set} = \begin{pmatrix} \mathbf{0} & \mathbf{0} & \mathbf{0} \\ \mathbf{0} & \sigma_{lh}^2 + \sigma_{cent}^2 + \sigma_p^2 & \mathbf{0} \\ \mathbf{0} & \mathbf{0} & \sigma_{lv}^2 \end{pmatrix} \quad (8)$$

The last two error sources in the above classification that are the measurement error and the laser beam width can be estimated by C_{int} is the covariance matrix that is a combination of noise measurement and laser beam width:

$$C_{int} = C_b + C_{obs} \quad (9)$$

In which $C_b = \text{diag}(0, \sigma_b^2, \sigma_b^2)$, $C_{obs} = \text{diag}(\sigma_\rho^2, \sigma_\alpha^2, \sigma_\theta^2)$, σ_ρ is uncertainty of range; $\sigma_\alpha, \sigma_\theta$ are uncertainties of horizontal and vertical angles. $\sigma_b = \pm \delta/4$ with δ is the diameter of laser cross-section in angular units.

Finally, the uncertainty of the measured point cloud (covariance matrix C_x) can be computed by a law of error propagation of both the estimated georeferencing parameters and scanner observations. The covariance matrix C_x can be computed as (Scaioni, 2005):

$$C_x = J_{geo} C_{geo} J_{geo}^T + J_\rho C_{int} J_\rho^T \quad (10)$$

Where: J_{geo} and J_ρ are Jacobian matrix; C_{geo} is the covariance matrix of estimated parameters depending on the accuracy of targets in GCPs and geometry configuration between the scan station and targets.

3. Experiments

The experimental object is a façade of five-story and two-story buildings located on the main



Figure 3. Field work experiments in HUMG.

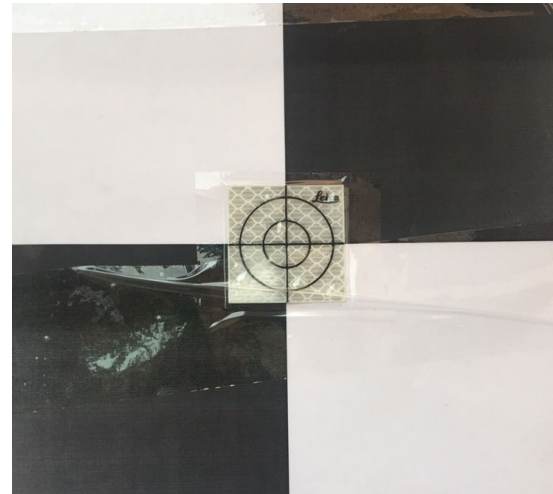


Figure 4. Checkered target with a reflective sheet.

campus of Hanoi University of Mining and Geology (HUMG) on 10th November 2021 (Figure 3).

Some main steps for these experiments will be presented in the following:

Control network. A traverse network including 6 control points was established, in which there were four new points (B, C, D, and E) and two reference points (A and F). The coordinates of these points are measured by a Leica TS06 plus total station in the VN-2000

coordinate system. The diagram of the traverse configuration is shown in Figure 5.

Because the existing ground control points are not adequate for the resection, some checkered targets are used. Fourteen checkered targets (Figure 5) were placed on the wall of buildings and their coordinates were measured by the Leica TS06 plus the total station. To improve the accuracy, each checkered target was added with one reflective sheet at its center

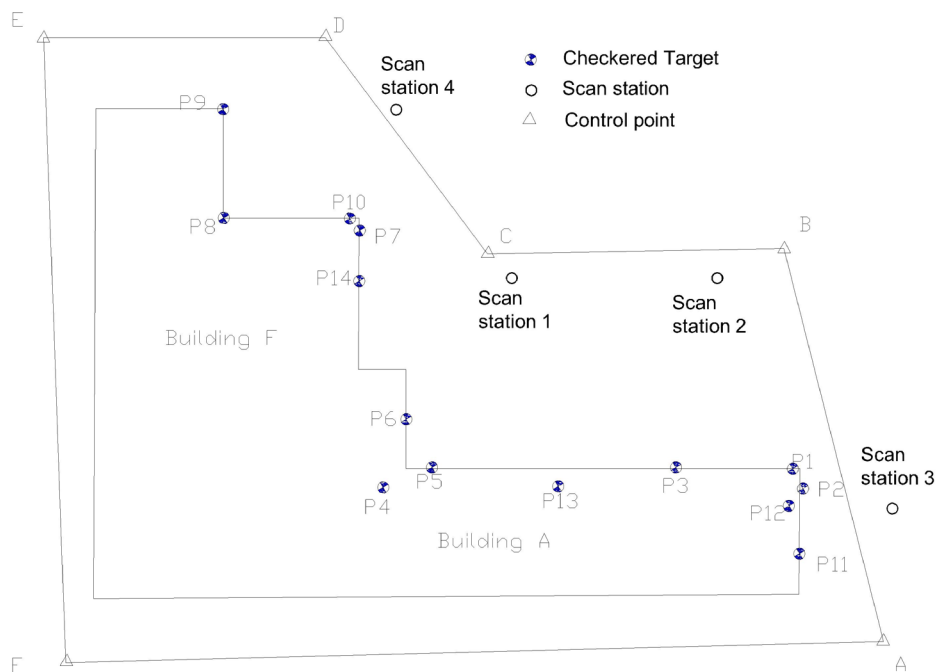


Figure 5. Plan of the experiment area at HUMG campus.

(Figure 4). In addition, the coordinates of checkered targets were averaged from at least two separate control points.

Resection method. In direct georeferencing, the coordinates of scan stations need to be determined in fieldwork. The resection is one of the methods that can obtain the coordinates of the scan station. Theoretically, the 3D resection method uses at least two control points to compute the coordinates of the stations (Breach, 1994). In this study, the coordinate of the scan station was determined by the resection using three or more control points by the total station unit of GTL-1000. An example of the resection configuration is given in Figure 2. The backsighting target is also chosen in the same way in common geodetic methods that should be a clear image and considerable far from the scanner.

In these experiments, at scan stations 1 and 2, the checkered targets P13 and P3 are selected since the distances from these targets to the scanner are long enough. Additionally, the faces of these targets are perpendicular to the direction of the scanner for pointing more accurate.

Scanner. The scanner used for this experiment was the scan unit of GTL-1000. The specifications of this instrument relevant to the scan unit are shown in Table 1. The instrument resolution was set at 11 mm at 10 m of range from the scanner to the surveyed object. In these experiments, the ranges are about from 20m to less than 50 m. The software Magnet Collage was

used for the processing of the scan data. In the experiment, one face of A and F buildings was scanned. A total of four stations were used to complete the surveyed area as illustrated in Figure 5.

Total uncertainties of a point cloud. As mentioned in Section 2, the total uncertainty of a point cloud includes the uncertainties of control points, resection procedure, observations of scans and other possible sources.

The uncertainty of point clouds, as specified in this paper, is based on the relative position of two point clouds of a similar object from two individual scan stations. The difference between two the point could be measured by the distance between them. The software Cloudcompare V2.6.3 was applied in which the distance is computed by the Cloud-to-Cloud method. The idea behind this method is that the distance is calculated from one point in the compared cloud to the nearest point in the reference cloud. More details of the Cloud-to-Cloud (C2C) method can be found in (Lague et al., 2013). In this experiment, the reference cloud is selected by the point cloud of nearer scan stations. Because the distance and incidence angle from the scan station to the surface's object is shorter, the density of the point cloud is higher.

In the experiment, sixteen test sites were carried out as depicted in Figure 6. To investigate the total uncertainty of point cloud, the test site (7) is used since the surface of scanned object is nearly perpendicular to the laser beam. The range

Table 1. Specifications for Scan Unit and Camera of GTL-1000.

Scan unit	
Scanning data rate	Maximum of 100,000 points per second
Laser classification	Class 1
Wave length	870 nm
Resolving power	
Point increment	Fine 11mm (at 10 m) Standard 22mm (at 10m)
Field of view	V: 270 degree/ H: 360 degree
Range of measurement	0.6 to 70m
Distance accuracy	4 mm at 10 m; 6 mm at 20 m; 8 mm at 30 m
Surface accuracy	3 mm at 10 m; 5 mm at 20 m; 7 mm at 30 m
Coordinate accuracy	5 mm at 10 m; 7 mm at 20 m; 10 mm at 30 m
Camera	
Field of view	V: 270 degree/ H: 360 degree
Number of effective pixels	5M pixel

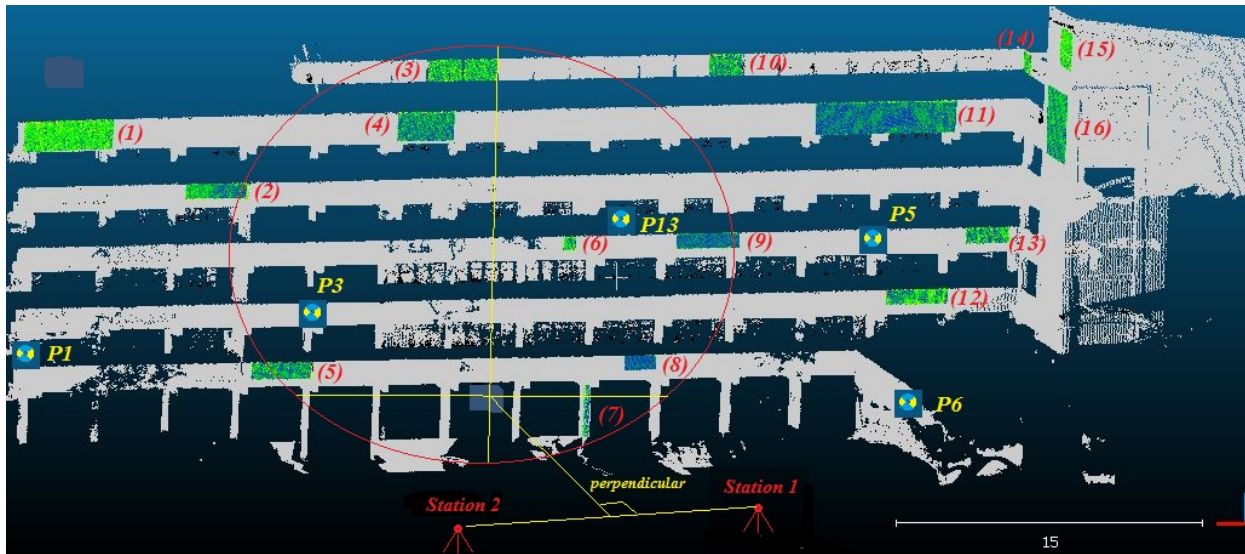


Figure 6. Relationship between the position of test sites and scan stations.

Table 2. The coordinates of control points and their accuracies.

Reference points	New points	North (m)	East (m)	Height (m)	Position RMSE (m)	Height RMSE (m)
A		2331107.288	580277.171	8.388	----	----
	B	2331149.205	580266.540	8.639	0.000	0.000
	C	2331148.616	580234.914	8.659	0.001	0.001
	D	2331171.693	580217.571	8.451	0.001	0.000
	E	2331171.715	580187.563	8.456	0.001	0.000
F		2331105.045	580189.911	8.536	---	---

and the incidence angle from the scanner to the surface are about 20 m and 20°, respectively. The test site (7) was taken place because the influence of the given incidence angle on the quality of point cloud is small.

Investigation of range and incidence angle on the uncertainty of point cloud. The range and incidence angle are the main factors influencing the uncertainty of the scanner’s observation including range, horizontal and vertical angles . These factors also influence the uncertainty of a point cloud (Reshetyuk 2009). The uncertainty of the scanner’s observations of TLS can be estimated by its specifications (Table 2). The incidence angle is defined as the angle between the laser beam vector and the normal vector of the surface.

To investigate the influence of the range and incidence angle on the quality of the point cloud, 16 subsets of the point cloud were selected for comparative analysis. These sites were

distributed around the façade of the building as shown in Figure 6. The locations of these sites lead to differences in the scan range and incidence angle.

4. Results

This study aims to analyze the influence of several error sources in the resection method on the quality of a point cloud. The uncertainty of a point cloud affects by the uncertainty of the control network, resection method including backsighting, the scan station setup, scanner’s observations, and possibly geometry configuration. This section will analyze the effect of each error source on the quality of the point cloud.

4.1. Accuracy of the control network

The control network was adjusted by using the least square method. The accuracy of the

control point is ≤ 1 mm according to both horizontal and vertical axis, as listed in Table 2. 14 checkered targets were placed around the study area as illustrated in Figure 4. The accuracy of these points in both horizontal and vertical components was from 1 to 2 mm.

4.2. Accuracy of resection method

Resection is one of the common methods for direct georeferencing in TLS. The positional accuracy of the scan station by using the resection method can be found in (Breach, 1994). In this experiment, the positional accuracy is < 3 mm in each direction (x, y, z). Figures 9 (a) and (b) show the accuracy of the scanner's position at stations 1 and station 2, respectively. The positional accuracies in stations 3 and 4 are similar to those of stations 1 and 2 but they are not shown here due to the limitation of paper. The error of pointing the backsight target equals $0.5''$ or 0.5 mm at 20 m which is computed by $\sigma_p = \pm 60''/M$ with M is telescope magnification $M=30X$.

4.3. The total uncertainty of a point cloud

From Table 3, the distance between two point clouds of two corresponding scanings at the test site (7) is 11.6 mm. If the uncertainties of two individual scanings are assumed to be comparable then the uncertainty of each scanning is $11.6/\sqrt{2}= 8.2$ mm. In the experiment, the uncertainties of control point, resection procedure, coordinates (Table 1) and, backsighting are about 3, 4, 7 and 0.5 mm, respectively. The amount of total error that can be computed by the law of error propagation is $\sqrt{3^2 + 4^2 + 7^2 + 0.5^2} = 8.6$ mm. It is worth noting that in the above computation the rotation matrix R_{IRS}^{GCP} is assumed to be the identity matrix because of a 20° of azimuth.

4.4. Influence of range and incidence angle on the point cloud

The influence of range and incidence angle on the uncertainty of point cloud is evaluated on 16 test sites shown in Figure 6. The probability characteristic of the distance is presented by mean value and standard deviation (STD) in Figure 7. Table 3 summarizes the maximum range, maximum incidence angle, mean value, and

Table 3. Properties of test sites and the mean and STD of range between two point clouds.

D: range; IA: incidence angle

Test sites	D (m) Max	IA ($^\circ$) Max	Mean value (mm)	STD (mm)
1	44	60	26.3	9.8
2	35	51	21.4	10.9
3	29	45	15.9	6.4
4	30	40	14.0	5.4
5	25	37	12.9	5.4
6	23	27	11.8	4.6
7	21	22	11.6	4.8
8	23	27	11.5	4.8
9	27	37	14.7	5.3
10	29	45	16.4	6.7
11	40	56	23.1	9.5
12	37	56	22.5	9.3
13	42	60	26.8	11.7
14	46	61	26.3	10.3
15	46	60	27.1	8.6
16	43	50	22.9	7.2

STD. In which, the maximum range is the larger range from two scan stations 1 and 2 to the test sites. Similarly, the maximum incidence angle is the larger angle from two scan stations 1 and 2 to the test sites.

The mean value and STD of the distance between two point clouds are illustrated in Figure . Both mean value and STD are small according to the test sites in the middle of the building (e.g., from the test site (3) to the test site (10)). The mean value and STD are smaller than 16 mm and 7 mm respectively. By contrast, these values significantly increase nearly twofold according to test sites on the left and right hand-side of the building.

Figures 11 and 12 illustrate the relationship between the mean value, STD and the range (r). A non-linear function can be established that is a downward parabolic curve. The coefficient of determination (R^2) used to measure these relationships that are 0.95 and 0.73, respectively.

Similarly, the relationship between the mean value, STD and the incidence angle can be established by a non-linear function. Upward

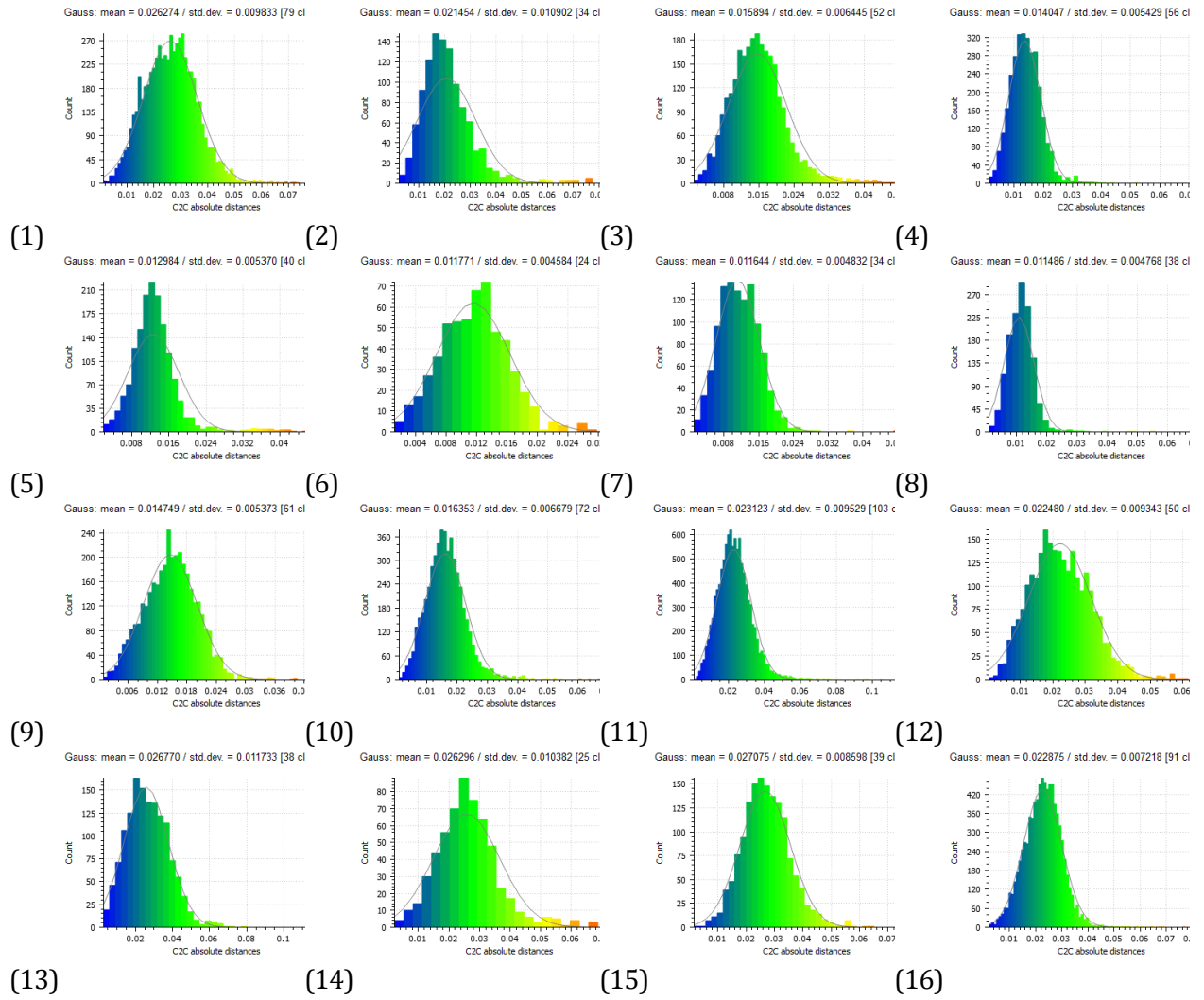


Figure 7. Mean value and standard deviation of the distance between two point clouds.

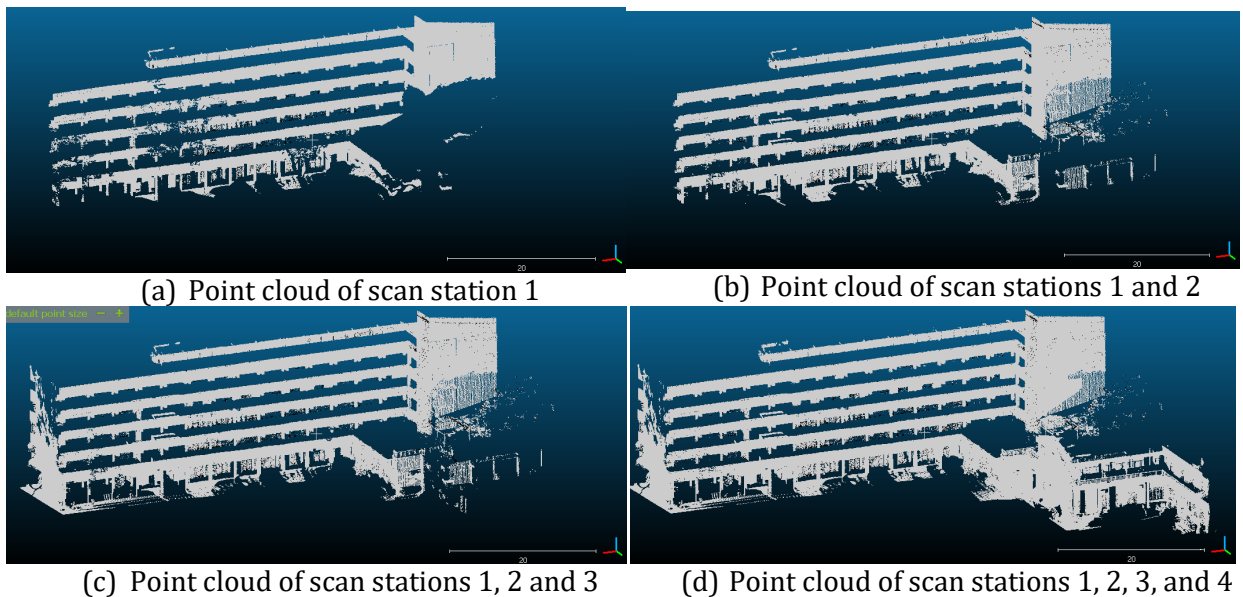


Figure 8. The point cloud of building's surface from four separate scan stations using resection method.

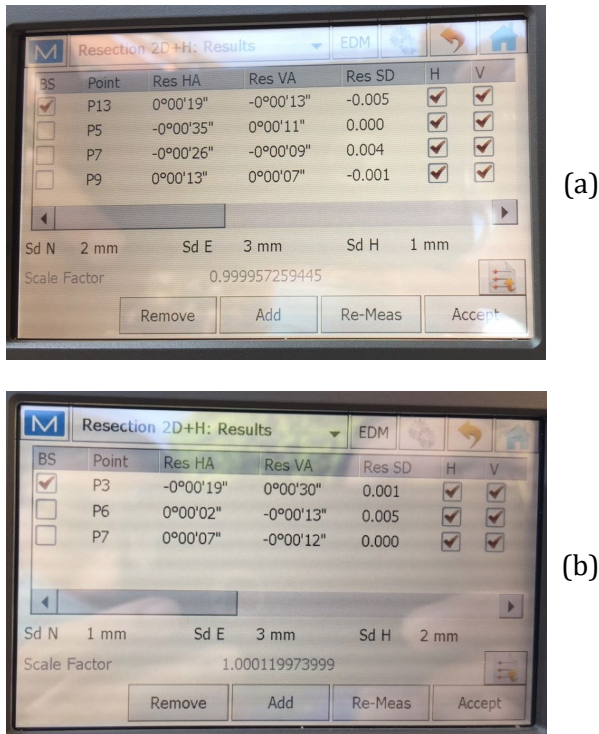


Figure 9. An example of resection accuracy at the scan station 1 (a) and the scan station 2 (b).

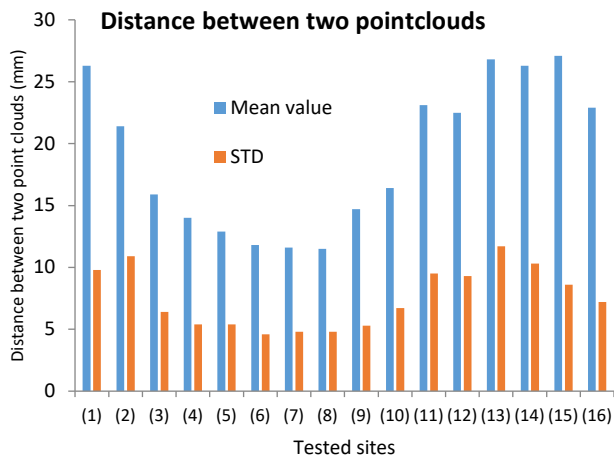


Figure 10. Mean value and STD of distance between two point clouds computed by C2C.

parabolic curves are used and the R^2 values are 0.97 and 0.84 shown in Figures 13 and 14.

Finally, Figure 8 plots the point cloud of the surface of A and F buildings contributed from separate point clouds of four scan stations. The whole point clouds of buildings can be shown after finishing scanning a few minutes in the

fieldwork. The registration and georeferencing procedures in the office are no longer to use.

5. Discussions

The experimental result agrees with the theory about the total uncertainty of the point cloud of the resection method as mentioned in section 2. The total uncertainty of a point cloud measured by the resection method influences the uncertainty of the control point, resection procedure, backsight, and scanner observations. However, the most influencing factor contributing to the total error is observations of the scanner (distance and horizontal and vertical angles).

Both the range and incidence angle are the main factors influencing the quality of the point cloud. Regarding the test sites in the middle of the building, the influence of these factors is relatively small since the range from the scan station to the test sites is smaller than 30 m and the incidence angle is smaller than 45° . This means that the uncertainty of range and diameter of laser cross-section is relatively small. So that the uncertainty of the point cloud is small. Whereas regarding the test sites on both sides of the building, the range increases upto about 46 m and the incidence angle grows to 60° . Both uncertainty of range and laser beam width (diameter of laser cross-section) increase. The beam width is a considerable error source that is described in equation (9). That leads to the increasing uncertainty of the point cloud. These results are consistent with the previous result (Lichti and Gordon, 2004) that the beam width uncertainty is an influencing factor.

The downward and upward parabolic curves for the relationship between the mean and STD and the range (r) and incidence angle (IA) are suitable. These results can be explained by the characteristics of the uncertainty in range using the principle of electronic distance measurement. This issue can be seen in the distance accuracy item in Table 1. By contrast, the uncertainty of scanner measurements slightly increases with small incidence angles but significantly increases with large incidence angles. These results are in agreement with the investigation of the relationship between incidence angle and measurement (Soudarissanane et al., 2009).

The resection method allows us to generate the surface of a complex building from several

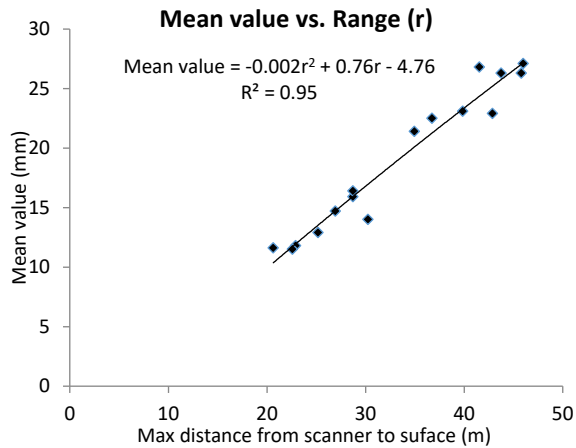


Figure 11. Coefficient of determination of the relationship between the mean value and the range.

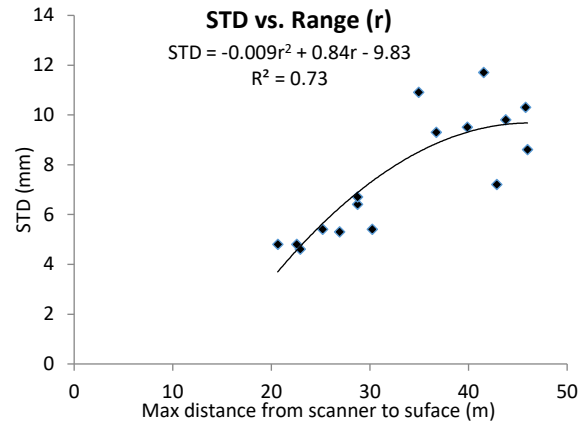


Figure 12. Coefficient of determination of the relationship between STD and the range.

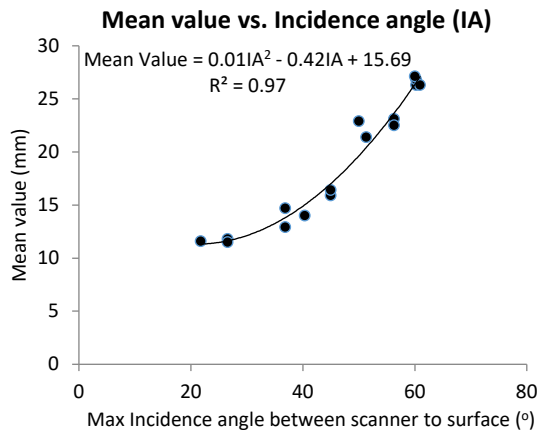


Figure 13. Coefficient of determination of the relationship between the mean value and IA.

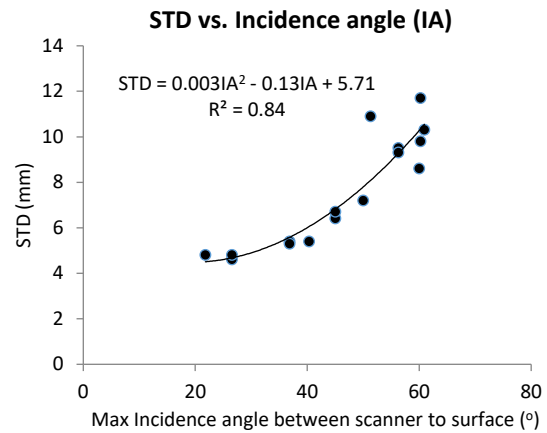


Figure 14. Coefficient of determination of the relationship between STD and IA.

scan stations without registration. This is the most advantage of the resection method by significantly saving time for data post-processing in the office. The scan data of a complex surveyed object can show and check during or after finishing the scanning. In addition, the high accuracy of the scanner's coordinate achieved from the resection method is able to combine separate point clouds from corresponding individual stations. But, to carry out the resection method, a control network need to be established before scanning. This is the main drawback of the resection method used for direct georeferencing in TLS.

Finally, the resection method for determining the scanner position is suitable to apply in the

field of civil engineering since a control network existed in the scanned area in the previous stages.

6. Conclusions

The resection method is one of the most suitable methods for direct georeferencing in TLS which can be summarized as the following:

The direct georeferencing using the resection method is sufficiently accommodated the high accuracy. The millimeter level in accuracy of scan station's coordinates obtained by the resection method is an outstanding benefit in the direct georeferencing compared to the centimeter level of GNSS-RTK. In addition, the scan station using resection is free which is another benefit

compared to the GNSS method due to multipath effects.

Besides, the direct georeferencing using the resection method help to reduce the time for data processing. Coordinates of scan stations are measured by the resection method so that the point cloud from separate scan stations are located in the global coordinate without both the registration and georeferencing. Moreover, the completeness of scan data can be checked in the field.

An important finding in this study is the relationship between the uncertainty of scan observations and the range and incidence angle. These results suggest that both the range and incidence angle from the scanner to the surveyed object are the main factors influencing the uncertainty of the point cloud.

However, the potential limitation of the resection method in georeferencing is that it needs an existing control network in the surveyed area.

In future works, other influencing factors on the quality of point cloud should be investigated.

Acknowledgments

This paper has been funded under the research program T21-20 of Hanoi University of Mining and Geology.

Contribution of authors

Dung Trung Pham contributes to the idea, data acquisition and analysis, and writes the manuscript; Cuong Xuan Cao contributes to edit the writing; Anh Tuan Nhu Nguyen, Tinh Duc Le, Canh Van Le, and Cuong Sy Ngo contribute to collect the data.

References

- Altuntas, C., Karabork, H., & Tusat, E. (2014). Georeferencing of ground-based LIDAR data using continuously operating reference stations. *Optical Engineering*, 53(11), 114110.
- Breach, M. (1994). Three dimensional resection. *Surveying and Land Information Systems*, 54(1), 21-25.

Hofmann-Wellenhof, B., Lichtenegger, H., & Wasle, E. (2007). *GNSS—global navigation satellite systems: GPS, GLONASS, Galileo, and more*. Springer Science & Business Media.

Jaud, M., Letortu, P., Augereau, E., Le Dantec, N., Beauverger, M., Cuq, V., Prunier, C., Le Bivic, R., & Delacourt, C. (2017). Adequacy of pseudo-direct georeferencing of terrestrial laser scanning data for coastal landscape surveying against indirect georeferencing. *European Journal of Remote Sensing*, 50(1), 155-165.

Lague, D., Brodu, N., & Leroux, J. (2013). Accurate 3D comparison of complex topography with terrestrial laser scanner: Application to the Rangitikei canyon (NZ). *ISPRS journal of photogrammetry and remote sensing*, 82, 10-26.

Lichti, D., & Gordon, S. (2004). *Error Propagation in Directly Georeferenced Terrestrial Laser Scanner Point Clouds for Cultural Heritage Recording*.

Reshetyuk, Y. (2009). *Self-calibration and direct georeferencing in terrestrial laser scanning*, KTH.

Scaioni, M. (2005). Direct georeferencing of TLS in surveying of complex sites. *Proceedings of the ISPRS Working, Group 4*, 22-24.

Schuhmacher, S., & Böhm, J. (2005). Georeferencing of terrestrial laserscanner data for applications in architectural modeling 3D-ARCH 2005. *Virtual Reconstruction and Visualization of Complex Architectures*. XXXVI, part 5: W17.

Soudarissanane, S., Lindenbergh, R., Menenti, M., & Teunissen, P. (2009). Incidence angle influence on the quality of terrestrial laser scanning points. *Proceedings ISPRS Workshop Laserscanning 2009*, 1-2 Sept 2009, Paris, France.

Zimmermann, F., Holst, C., Klingbeil, L., & Kuhlmann, H. (2018). Accurate georeferencing of TLS point clouds with short GNSS observation durations even under challenging measurement conditions. *Journal of Applied Geodesy*, 12(4), 289-301.